Editorial Manager(tm) for Neuroscience
Manuscript Draft

Manuscript Number:

Title: Environmental enrichment selectively increases glutamatergic responses in layer II/III of the auditory cortex of the rat

Article Type: Research Paper

Section/Category:

Keywords: Behavior, AI, Patch-clamp, perforated patch, excitation/inhibition balance, neuronal modeling

Corresponding Author: Dr. Marco Atzori, PhD

Corresponding Author's Institution: University of Texas at Dallas

First Author: Justin A Nichols, doctoral student

Order of Authors: Justin A Nichols, doctoral student; Vikram Jakkamsetti, doctoral student; Lu Dinh, doctoral student; Michael P Kilgard, associate professor; Marco Atzori, PhD

Manuscript Region of Origin:

Abstract: Prolonged exposure to environmental enrichment (EE) induces behavioral adaptation accompanied by detectable morphological and physiological changes. Auditory EE is associated with an increased auditory evoked potential (AEP) and increased auditory gating in the primary auditory cortex. We sought physiological correlates to such changes by comparing synaptic currents in control vs. EE-raised rats, in a primary auditory cortex (AI) slice preparation. Pharmacologically isolated glutamatergic or □-amino-butyric acid-A (GABAA-) receptor-mediated currents were measured using perforated patch whole-cell recordings. Glutamatergic alpha-amino-3-hydroxy-5-methyl-4-isoxazolepropionic acid-receptor- (AMPAR-) mediated postsynaptic currents (EPSCs) displayed a large amplitude increase (64.2 ± 11.6 % in EE vs. control) accompanied by a rise-time decrease (-29.24 ± 5.7 % in EE vs. control) and decrease in pair pulse ratio in layer II/III but not in layer V. Changes in glutamatergic signaling were not associated with changes in

the ratio between N-methyl-D aspartate-receptor- (NMDAR-) mediated vs. AMPAR- mediated components, in amplitude or pair pulse ratio of GABAergic transmission, or in passive neuronal properties.

A realistic computational model was used for integrating in vivo and in vitro results, and for determining how EE synapses correct for phase error of the inputs. We found that EE not only increases the mean firing frequency of the responses, but also improves the robustness of auditory processing by decreasing the dependence of the output firing on the phase difference of the input signals.

We conclude that behavioral and electrophysiological differences detected in vivo in rats exposed to an auditory EE are accompanied and possibly caused by selective changes in cortical excitatory transmission. Our data suggest that auditory EE selectively enhances excitatory glutamatergic synaptic transmission in layer II/III without greatly altering inhibitory GABAergic transmission.

Dear Dr. Lisberger and Dr. Quirk,

please, receive our manuscript entitled "**Environmental enrichment selectively increases glutamatergic responses in layer II/III of the auditory cortex of the rat**" for review and publication on "Neuroscience".

We used a model of auditory enriched environment to investigate possible neocortical synaptic changes associated with it. The model has been widely tested in other studies by some of us, who also demonstrated previously that environmental enrichment produces large changes in scalp recording from enriched rats. A natural follow up of those studies was to determine the cellular bases of such changes.

We used patch clamp recording for monitoring synaptic currents, overcoming the problem of the relative old age of the animals -due to the enrichment protocol- with the perforated patch technique, which allowed us to record from animals up to several-month old. Our main finding is that environmental enrichment is accompanied by several changes in glutamatergic synaptic responses, while the inhibitory, GABAergic system, did not show any measurable changes following the same treatment. Most notably, the amplitude of synaptic glutamatergic currents in enriched animals was more than 60% larger than in control animals.

Many works studied the behavioral consequences of living in a sensory enriched environment, but only a handful of them report its correlates at the neural level. Most, if not all of them, deal with changes at the level of the hippocampus, for its obvious relevance in learning and memory. To our knowledge, ours is one of the first studies to report on neural modifications at the neocortical single cell level.

We also used a Hodgkin-Huxley model of neurons for constructing two simple neural networks to better understand the computational consequences of environmental enrichment. The first part of the model suggests an explanation for the "increased gating", terminology referring to the increase in pair pulse depression observed by some of us in *in vivo* recordings from enriched animals. The second part of the model shows that environmental enrichment not only produces a solid increase in the responses in terms of firing frequency, but it also increases the robustness of the network by making it less sensitive to differences in the phase of the input layer.

We believe that our study will pave the ground to further studies on the cortical effects of the environmental enrichment. We did not insert the source MatLab codes used for the simulations. In case you would like to have them we will be glad of letting you and your journal have them.

The manuscript is not under revision in any other journal and the material has only been presented earlier under the form of abstract or poster. The manuscript is in accordance with the statement of ethical standards for manuscripts submitted to *Neuroscience.*

thanking you for your attention, we send you our
Best regards

Marco Atzori and co-authors

Marco Atzori
Assistant Professor
The University of Texas at Dallas/GR41
Richardson, TX 75080
tel. 972 883 4311
fax 972 883 2491
marco.atzori@utdallas.edu

*** 2 - Reviewer Suggestions**

We would like to suggest the following reviewers:

Mark Murphy
Phone: 61-3-8344 5785
Fax: 61-3-9347 5219
Email: m.murphy@unimelb.edu.au
Department of Anatomy and Cell Biology
The University of Melbourne
Victoria 3010 Australia

Hubert H R O Dinse
Ruhr Univ Bochum
Inst Neuroinformatik
Lehrstuhl Theoretische Biol ND04 Box 102 148
D-44780 Bochum
Germany
Work Phone: 492343225565
Fax: 492343214209
E-mail: HUBERT@NEUROINFORMATIK.RUHR-UNI-BOCHUM.DE

Michael E Hasselmo, PhD
Boston Univ
Psych Ctr Mem & Brain
2 Cummington St
Boston MA 02215
work phone: 617-353-1397
fax: 617-353-1424
e-mail: hasselmo@bu.edu

Environmental enrichment selectively increases glutamatergic responses in layer II/III of the auditory cortex of the rat.

Justin Nichols, Vikram Jakkamsetti, Lu Dinh, Michael Kilgard, Marco Atzori*

The University of Texas at Dallas
School for Behavioral and Brain Sciences

***Corresponding author**:

Marco Atzori
2601 N. Floyd road
GR41
University of Texas at Dallas
School for Behavioral and Brain Sciences
Richardson, TX 75080

Field editor

Behavioral Neuroscience:
Dr. G.J. Quirk, Ponce School of Medicine
Department of Physiology
Dr. Ana Marchand Perez Street
Urb. Industrial Reparada, Ponce, 00731, Puerto Rico

Abbreviations: AI, primary auditory cortex; ACSF, artificial cerebrospinal fluid; AMPA, α-amino-3-hydroxy-5-methyl-4-isoxazolepropionic acid; APV, D-2-amino-5-phosphonopentanoic acid; eEPSC, evoked postsynaptic current; $GABA_AR$, γ-aminobutyric acid A receptor; NMDAR, N-methyl-D-aspartate receptor; DNQX, 6,7-Dinitroquinoxaline-2,3-dione

Abstract

Prolonged exposure to environmental enrichment (EE) induces behavioral adaptation accompanied by detectable morphological and physiological changes. Auditory EE is associated with an increased auditory evoked potential (AEP) and increased auditory gating in the primary auditory cortex. We sought physiological correlates to such changes by comparing synaptic currents in control vs. EE-raised rats, in a primary auditory cortex (AI) slice preparation. Pharmacologically isolated glutamatergic or γ-amino-butyric acid-A ($GABA_A$-) receptor-mediated currents were measured using perforated patch whole-cell recordings. Glutamatergic alpha-amino-3-hydroxy-5-methyl-4-isoxazolepropionic acid-receptor- (AMPAR-) mediated postsynaptic currents (EPSCs) displayed a large amplitude increase (64.2 ± 11.6 % in EE vs. control) accompanied by a rise-time decrease (-29.24 ± 5.7 % in EE vs. control) and decrease in pair pulse ratio in layer II/III but not in layer V. Changes in glutamatergic signaling were not associated with changes in the ratio between N-methyl-D aspartate-receptor- (NMDAR-) mediated vs. AMPAR- mediated components, in amplitude or pair pulse ratio of GABAergic transmission, or in passive neuronal properties.

A realistic computational model was used for integrating *in vivo* and *in vitro* results, and for determining how EE synapses correct for phase error of the inputs. We found that EE not only increases the mean firing frequency of the responses, but also improves the robustness of auditory processing by decreasing the dependence of the output firing on the phase difference of the input signals.

We conclude that behavioral and electrophysiological differences detected *in vivo* in rats exposed to an auditory EE are accompanied and possibly caused by selective changes in cortical excitatory transmission. Our data suggest that auditory EE selectively enhances excitatory glutamatergic synaptic transmission in layer II/III without greatly altering inhibitory GABAergic transmission.

Key words

Behavior, AI, Patch-clamp, perforated patch, excitation/inhibition balance, neuronal modeling

The anatomic connectivity and physiological properties of the central nervous system are determined by a combination of genetic programs and by the type and amount of sensory input (Bartoletti et al., 2004). Many studies report anatomical and cellular consequences of the exposure to a sensory enriched environment (EE).

While several studies reported the effects of EE on synaptic transmission in the hippocampus (Duffy et al., 2001; Artola et al., 2006; Irvine and Abraham, 2005; Foster and Dumas, 2001), scant information is available on the effects of EE on the synaptic properties of the neocortex. In a previously developed model of auditory EE Engineer et al. demonstrated large increases in surface AEPs and in the number of action potentials recorded at the auditory cortex (Engineer et al., 2004). EE also increased the degree of auditory gating (paired pulse depression) recorded with both epidural and intracortical electrodes (Percaccio et al., 2005). Physiological differences detected in the auditory cortical responses might originate in the cortex itself, or might rather be the result of a different subcortical processing between control and EE animals. The purpose of this study was to identify a possible local, cortical source of differential processing between control and EE animals. We used the same behavioral paradigm of auditory EE reported above (Engineer et al., 2004; Percaccio et al., 2005) to investigate differences in pharmacologically isolated excitatory and inhibitory synapses in EE vs. control-raised animals in the auditory cortex of the rat.

Experimental Procedures

Environmental conditions

Twenty-three control and twenty-seven EE-raised Sprague-Dawley rats were used in this study. All rats were housed with their mothers and littermates until they reached an age of twenty-one days. They were then randomly separated and placed into either enriched or standard housing conditions. Rats were given a code of colored tail stripes in order to preserve their housing condition's confidentiality from experimenters and avoid any unintentional bias. All rats were provided with food and water *ad libitum*. A reverse twelve hour light/dark cycle and constant humidity and temperature was maintained for both groups. All experimental procedures were performed in accordance with the NIH Ethical Treatment of Animals and were approved by the University Committee on Animal Research at the University of Texas at Dallas. Housing conditions were nearly identical to those described in previous studies (Percaccio et al., 2005; Engineer et al., 2004). The enriched environment (EE) exposure time for this study averaged 5 weeks.

Four to eight rats were housed together in the EE cage which was located in a separate room from the main rat colony at UTD. This cage (76 X 45 X 90 cm) had four levels accessible by ramps. The environment's complexity was augmented by bells, wind chimes, and chains. Tones at 2.1 or 4.0 kHz were sounded when touch plates (located at the bottom of two of the ramps) were depressed. Additionally a chime was sounded when an infrared beam was broken in front of the water source and each rotation of an exercise wheel activated a small green light emitting diode and a 3 kHz tone. These devices were designed and positioned in such a way that their sounds provided information about movement in a specific location within the cage at a particular time.

Other meaningful sounds were provided by a CD player. Every 2 – 60 seconds, a randomly selected sound was played, including simple tones, amplitude and frequency

modulated tones, noise bursts, and other complex sounds (rat vocalizations, classical music, rustling leaves, etc.). Seven of the seventy-four sounds activated a pellet dispenser (Med Associates) that delivered a sugary treat intended to encourage attention to the sounds. The rewarded tracks included interleaved tones of different carrier frequencies (25 ms long and 4, 5, 9, 12, 14, and 19 kHz tones with inter-stimulus intervals ranging from 50 ms to 2 seconds) and frequency modulated sweeps (1 octave up or down in a 140 or 300 ms sweep with inter-stimulus intervals ranging from 80 to 800 ms). All sounds were < 75 dB SPL, provided 24 hours a day and spanned the entire hearing range of the rat (1-45kHz).

Standard environment cages were 26 X 18 X 18 cm and included 1-2 rats per cage. The standard housing environment exposed rats to vocalizations from 20 - 30 other rats housed in the same room, in addition to general sounds (which were also heard by rats in the EE) resulting from daily traffic, cleaning, and feeding while they were most active. Although rats housed in both environments heard approximately the same number of sounds each day, sounds in the EE condition were more diverse, and provided more behaviorally significant information than the sounds in the standard condition.

Slice preparation

We followed an auditory cortex slice preparation protocol similar to one previously described (Atzori et al., 2001). After exposure to enriched or standard environmental conditions (as described above), six to nine week old Sprague Dawley rats were anesthetized (evaluated by toe-pinch response) in a chamber with vaporized isoflurane (0.2ml/100g) and immediately decapitated. The brains were carefully

extracted and immersed in a solution (slicing ACSF) chilled to approximately 0.5˚C containing (mM) 130 NaCl, 3.5 KCl, 10 Glucose, 24 $NaHCO_3$, 1.25 NaH_2PO_4, 0.5 $CaCl_2$ and 1.5 $MgCl_2$, and saturated with a mixture of 95% O_2 and 5% CO_2 (pH ≈ 7.35 osmolarity 301 ± 5mOsm). After removal of the cerebellum, a vibratome (VT1000, Leica, Germany) was used to cut 270 μm-thick coronal slices from the first sixth of the caudal part of the brain, corresponding to the primary auditory area (A1). Slices were then placed into an incubating chamber super-fused with the ACSF solution described above and incubated at 33˚C for approximately one hour, and then maintained at room temperature until used for recording.

Electrophysiology

Slices were transferred to a recording chamber and immersed in a solution (recording – ACSF) similar to the slicing - ACSF solution described above containing 1.5 mM $CaCl_2$ rather than 0.5 mM. Pyramidal neuron selection procedures were adopted from those described previously (Atzori et al., 2005). Cells with an obvious apical dendrite located in layers II/III or V and dorsal to the ectosylvian region were visually selected using a Luigs & Neumann 380 FM Workstation with Olympus BX51 WI optics and an infrared camera system.

Perforated patch clamp recordings were performed using techniques similar to the whole cell patch clamp technique already described (Atzori et al., 2001), with an internal recording solution containing, in addition, the antibiotic amphotericin B (3.24 mM). Both intracellular recording solutions contained in mM 100 CsCl, 5 1,2-bis(2-

aminophenoxy)ethane-*N,N,N',N'*-tetraacetic acid K (BAPTA-K), 1 lidocaine *N*-ethyl bromide (QX314), 1 $MgCl_2$, 10 N-(2-hydroxyethyl)piperazine-N'-(2-ethanesulfonic acid) (HEPES), 4 glutathione, 1.5 $ATPMg_2$, 0.3 GTPNa2, 8 biocytin (pH ≈ 7.35 osmolarity 270 ± 10 mOsm). Amphotericin B was used to form pores in the neuronal membrane layer allowing electrical access (perforated-patch) without the intracellular dialysis normally associated with whole cell patch clamping. The pulled glass electrode tips (5-8 MΩ) were back filled with the intracellular recording solution after the most distal 200 μm were filled with the amphotericin B free intracellular solution in order to prevent tip clogging during electrode – membrane seal formation. Holding current (I_h) and input resistance (Ω_{in}) was continuously monitored with a 2mV negative pulse delivered before the paired pulse protocols. Recording was delayed until the voltage gated sodium channel blocker lidocaine (QX314) reached an intracellular concentration high enough to prevent action potentials and input resistance stabilized (15-20 min).

Electrically evoked post synaptic currents were measured by delivering two electric stimuli (90-180 μs, mean μA) 20, 40, 50, 100, 500, and 1000 ms apart every 8 seconds with a stimulus isolator (A365 triggered by a DS8000-82112 Digital Simulator, both from World Precision Instruments) through a glass stimulation mono-polar electrode filled with recording-ACSF, and always placed at the same distance (approximately 120 μm) from the recording electrode.

Excitatory post synaptic currents (EPSCs) were measured in a bath of bicuculline (10 μM) at a holding potential of - 60 mV for inward currents and + 60 mV for outward currents and reversibly blocked by DNXQ (10 mM) and Kynurenic acid (2 mM) indicating a glutamatergic composition. EPSC's amplitude was measured at the peak of

inward current as AMPA current (I_{AMPA}), and current amplitude 45 ms after the outward excitatory current peak was taken as the estimate of NMDA current (I_{NMDA}). Similar methods were previously described (Duffy et al., 2001). We selected the ratio between NMDA receptor mediated currents and AMPA receptor mediated currents (I_{NMDA}/I_{AMPA}) as an indicator of post synaptic function. Paired Pulse Ratio (PPR) was defined as the ratio between the mean of the second inward current response and the mean of the first inward current response (P_2/P_1).

Inhibitory post synaptic currents (IPSCs) were measured at a holding potential V_h = -60 mV in a bath solution containing 10 μM 6,7-dinitroquinoxaline-2, 3-dione (DNQX) and 2 mM kynurenic acid for blocking glutamate receptor-mediated currents. The intracellular recording solution provided a reversal potential for Cl^- of approximately 0 mV. Inhibitory postsynaptic currents (IPSCs) were blocked by bicuculline (10 μM), indicative of their GABAergic origin.

Signals were acquired via a Digidata 1322A 16 bit data acquisition system controlled by Clampex 9.2 and Multiclamp 700B software (Axon Instr., California) and filtered at 3200 Hz (low pass) with a Frequency Devices 900 tunable active filter. The recording chamber was situated within a 1 m^3 faraday cage on an anti-vibration table (Technical Manufacturing Corporation) attached to a dedicated ground. DNQX and amphotericin B were dissolved in dimethylsulphoxide (DMSO). All other drugs were dissolved in de-ionized H_2O. All drugs in this study were purchased from Sigma (St. Louis, MO, USA) or from Tocris (Ellisville, MO, USA).

Data analysis

Statistical analysis was performed with Clampfit 9.2, SigmaPlot 8.0, and Microsoft Excel software. A Student's unpaired t-test was used for comparison between different groups of cells. Data were reported as significantly different only if $p < 0.05$.

Neural model

We used MatLab to develop a realistic neural network model for simulating the effects of EE on cortical processing. The model, described in more detail in the appendix, used a three-compartment pyramidal neurons and a single compartment interneuron with previously described voltage-gated conductances (Wang, 1998). Synaptic release elicits α-function like synaptic currents (see the Results and Appendix sections). Short-term memory properties of the synapses (facilitation and fast and slow depression) are present in the model as reported previously (Brunel and Wang, 2001; Tiesinga and Sejnowski, 2001; Varela et al., 1997).

Results

AMPAR-mediated currents in layer II/III

Since EE increases 3H AMPA binding in the hippocampus (Foster et al., 1996) and has been suggested to enhance glutamatergic activity (Foster and Dumas, 2001), we first measured the amplitude of electrically evoked AMPA currents in visually identified

neurons from layer 2/3 of the auditory cortex. A paired pulse protocol was applied with an interpulse delay varying between 20 and 1000 ms, for evaluating possible presynaptic differences between EE and the control group. In order to avoid a possible bias due to different stimulation conditions, the distance between stimulation and recording electrode and the stimulation intensity were kept in a narrow range. All recordings were performed with the experimenter unaware of the rats housing condition. No significant changes in mean stimulation intensity were observed between groups (mean stimulation intensity was 3.91 ± 0.53 μA in control and 3.75 ± 0.32μA in EE). In these conditions, the amplitude of AMPAR-mediated current (I_{AMPA}) from environmental enriched (EE) animals was much larger in EE, compared to controls (I_{AMPA}(EE)/I_{AMPA}(control) = 64 ± 12 % (n = 10 in control and 11 in EE, representative traces in fig. 1A and B), suggesting that EE strongly enhances excitatory currents. Fig.1C and D report the mean as an excitatory postsynaptic currents (eEPSC) in control vs. EE animals and the mean of the stimulation intensity in the two conditions. Paired pulse ratio (PPR), calculated as the ratio between the second and the first responses (A_2/A_1) was measured at a series of interpulse intervals (IPIs) in the range 20 -1000 ms. EE animals had a lower PPR for IPI = 500 ms, ($P < 0.05$, n = 10 ctr, n = 11 EE, fig.1E). We also measured eEPSCs kinetics, finding that rise time in EE were 29 ± 6 % shorter with respect to control, while no difference was detected in the decay time (fig.1F and G respectively).

Altogether, these data suggest that EE alters glutamatergic synaptic responses in layers II/III.

GABAergic currents in layer II/III

The changes in extracellular signal associated with EE (Percaccio et al., 2005) might be due to an increase in excitatory drive and/or decreased inhibition. Decreased inhibition might be a consequence of a decrease in $GABA_AR$-mediated currents. We tested the hypothesis of a decrease in synaptic inhibition by directly measuring GABAergic currents (eIPSCs) from layer II/III neurons using a similar stimulation protocol to the one described in the previous paragraph, but in the presence of the glutamate ionotropic receptor blockers DNQX (10 μM) and kynurenic acid (2mM). The remaining currents were blocked by 10 μM bicuculline, confirming their GABAergic nature.

Evoked IPSCs amplitude was not different in control vs. EE animals (fig.2A). No difference in rise- or decay-time were detected (Fig. 2B and C). The same pair pulse protocol used for AMPAR-mediated currents (interpulse intervals in the range 20-1000 ms) was used to measure possible changes in PPR (Fig.2D). PPR too remained unchanged between the two conditions ($p > 0.5$, $n = 8$ each). These data suggest that changes in inhibition are not likely to play a major role in EE.

AMPA-mediated currents in layer V

The change in the AMPAR-mediated signals might be a selective, layer-specific change in synaptic strength, or might rather be associated with a generalized increase in synaptic function throughout the cortical mantle. For determining the specificity of the synaptic increase, we used the same protocol described previously for measuring the properties of AMPAR-mediated currents in layer V of the auditory cortex.

We could not detect any differences in synaptic strength, kinetic properties or PPR in ePSCSs recorded from layer V of the auditory cortex (n = 5 in control; n = 8 in EE). The results are displayed in fig.2 E,F,G and H.

Collectively, these results chapter indicate that the increase in AMPAR-mediated results detected in layer II/III, is synapse specific and layer specific.

I_{NMDA}/I_{AMPA}

Recent evidence highlighted that different types of glutamatergic synapses undergo a maturation process consisting in the activity-dependent insertion of AMPA receptors in a postsynaptic membrane initially containing only or prevalently NMDARs (silent synapse reviewed in (Isaac et al., 1999). We considered the hypothesis that EE would increase I_{AMPA} using a similar mechanism. To test this hypothesis we measured I_{AMPA} as well as NMDAR-mediated currents (I_{NMDA}) at the same synaptic connection, by first measuring I_{AMPA}, holding the membrane potential at V_m = -60 mV, and subsequently measuring I_{NMDA}, upon changing V_m to + 60 mV, in order to get rid of the Mg^{2+} block. An estimate of the ratio I_{NMDA}/I_{AMPA} was obtained by dividing the current measured at V_h = +60 mV

(45 ms after the stimulus artifact, to minimize the contribution of AMPAR-mediated currents), by the peak amplitude of the AMPA current (see *Experimental procedures*). No change was detected in the ratio I_{NMDA}/I_{AMPA}, indicating that changes in I_{AMPA} were accompanied by a proportional increase in I_{NMDA} (n = 6, control; n = 8 EE). A representative trace is shown in fig. 3A. Fig 3B shows the mean of the ratio I_{NMDA}/I_{AMPA}.

Neuronal models of the effects of EE

We built a realistic neuronal model of pyramidal cell and GABAergic interneuron, based on a set of conductances present in the two type of cells, discussed in more detail in the *Experimental procedures* section and in the Appendix, and used them to construct two minimal neural networks, modeling some possible consequences of the synaptic changes induced by EE.

1) increase in auditory gating

The model represented in fig.4A illustrates a network of two pyramidal (P) cells connected in series, plus a feed-forward GABAergic interneuron (I) connecting the input layer neuron (P1) with the output layer neuron (P2). Every synapse can be regarded as a large number of independent identical synapses impinging upon the same cellular target. We simulated the response of the network to two small square current pulses (10 ms) delivered at 100 ms interpulse delay, evoking one spike each in P1. In a particular set of cells, in the control situation, the two spikes induce a couple of facilitating, subthreshold synaptic responses both in P1 and I1 (fig.4B and C, black traces). The resultant synaptic

signal in P2 is not affected by the presence of I1 (fig.4D, black trace). In EE, because of the increase in excitatory synaptic strength and due to the facilitation at the glutamatergic synapse, a firing threshold is reached by I1, which fires at the second stimulus, resulting in the decrease of the second, but not the first synaptic signal detected in P2 (fig.4B, C, and D). The short delay associated with axo-somatic inhibition vs. axo-dendritic excitation contributes to minimize the time difference between the signal transiting in the di-synaptic (P1-I1-P2) or the monosynaptic (P1-P2) branches, increasing the contribution of inhibition to PPR.

In the real situation the signal is determined by the summation of the excitatory plus the inhibitory synaptic currents, which includes an unknown statistical distribution of firing and non firing interneurons. A reasonable possibility is that such distribution elicitis a modest PPR in control, substituted by a larger PPR in EE.

2) Enhanced robustness to input phase differences

One important property of auditory neurons is the capability to integrate oscillatory inputs with slight phase differences. We tested the hypothesis that auditory EE modifies the dependence of cell firing on input phase differences by using a neuronal network with two independent pyramidal neurons in the input layer (P1 and P2, fig.5A), and one pyramidal neuron in the output layer (P3). Two sinusoidal inputs at the same frequency with different phase are fed into P1 and P2 respectively (fig.5A). The amplitude of the sinusoidal was selected as to generate a minimal firing in the postsynaptic neuron (1 or 2 spikes), while the sum of the two inputs in phase generated a higher but still non-

saturated postsynaptic firing. We simulated the response of the system for three input frequencies (50, 20 and 5 Hz), in control or in EE (Fig. 5B,C and D).

As expected, the model showed that EE increases the mean firing frequency at all tested frequencies (fig.5 B,C and D). While at high stimulation frequency (i.e. 50 Hz, fig. 5B) the output firing frequency does not depend on the phase difference, at lower frequencies (i.e. 20 Hz, fig. 5C) in EE a small phase difference (≤ 30°) maximizes the firing frequency due to the increased interval for synaptic summation. At even lower frequencies (i.e. 5 Hz, fig.5D), in EE the increase in firing frequency associated with a small phase difference is conserved throughout the whole 180° phase interval as summarized in table 1.

Discussion

The influence of the environment on animal behavior has long been documented. Several anatomical and physiological studies have clearly demonstrated an involvement of the hippocampus and related structures (Green and Greenough, 1986; Foster et al., 2000; Sharp et al., 1985; Faherty et al., 2003; Foster and Dumas, 2001). Recently more attention has been focused on how EE affects other brain areas, including the neocortex (Nithianantharajah et al., 2004). In particular, large anatomical rearrangements of dendritic processing has been documented in the parietal cortex (Leggio et al., 2005), prefrontal cortex (Dierssen et al., 2003) as well as in monoaminergic neocortical innervation (Zhu et al., 2005; Hellemans et al., 2005). In the cat primary visual cortex,

EE has been found to be effective in rescuing ocular dominance columns impaired by dark rearing (Bartoletti et al., 2004). In the primary auditory cortex, EE induces major physiological rearrangements, detected as changes in single cell response properties as well as in scalp recording (Engineer et al., 2004; Percaccio et al., 2005).

Our results showed a strong and selective increase in amplitude and a change in kinetics of glutamatergic responses. These data are in agreement with the general increase in the excitability, firing rate and decrease in latency in the AEP amplitude observed in the response to short (25 ms) tones *in vivo* (Engineer et al., 2004).

The stability of the ratio between NMDAR-mediated and AMPAR-mediated currents indicates that EE is not associated with a selective insertion of new AMPARs in the postsynaptic membrane ("silent" synapse "awakening"). Yet, other postsynaptic changes preserving I_{AMPA}/I_{NMDA} might take place at EE synapses.

The dramatic increase in EPSC amplitude might simply reflect an increase in the total number of excitatory spines, in agreement with previous findings (Dierssen et al., 2003). Similarly, the lack of changes in eEPSC PPR at short (<500ms) II does not allow to exclude the presence of presynaptic rearrangements preserving PPR.

Unchanged inhibitory responses do not support a major role for inhibition in the EE-driven re-shaping of auditory cortical responses. A sharp-electrode study on hippocampal non-pharmacologically dissected synaptic currents reported similar conclusion (Foster and Dumas, 2001).

The increase in synaptic efficacy could be the result of a generalized synaptic strengthening or could be a layer-specific phenomenon. The unchanged excitatory responses from layer V would suggest the second hypothesis, indicating layer II/III as a

privileged substrate for the solidification of cortical plasticity. A similar conclusion was previously reached with an anatomical-morphological study (Johansson and Belichenko, 2002), and is expected if EE is caused by spike-time-dependent plasticity, since the threshold for action potentials in layer V is approximately 10 mV more positive than in layer II/III (Atzori et al., 2004).

The increase in synaptic amplitude after exposure to the EE might derive from the transformation of low-probability and small amplitude synapses into high probability, large amplitude synapses (Atzori et al., 2001). Yet, high probability synapses possess slower rise times and smaller PPR with respect to low-probability synapses, contrasting with our current finding that EE decreases rise-time and leaves PPR unchanged, suggesting a different origin for the synaptic changes in EE.

The use of a computational model corroborated the hypothesis that the increase in auditory gating in EE (Percaccio et al., 2005) is due in part or completely to local, cortico-cortical changes in excitatory synaptic strength.

Auditory information is largely conveyed by low frequency envelope signals surfacing onto AI with slight phase differences within an isofrequency contour. Our computational model showed that the synaptic changes associated with the EE not only produce an expectable increase in firing rate but that they also decrease the dependence of the postsynaptic firing rate on the input phase differences, in the case of two slow frequency de-phased inputs. In fact, at low input frequencies, the increase in firing rate corresponding to a small phase increase displayed in control is replaced in EE by a solid enhancement almost independent on the phase difference between the two inputs, making synaptic summation more robust in EE.

Although our data indicate that EE causes significant cortical plasticity, we cannot exclude the possibility that non cortical auditory relays are also modified by EE, introducing a further component to the EE-induced alteration of the cortical signal detected by AEP (Percaccio et al., 2005). In conclusion, we demonstrated for the first time that EE induces a change in the efficacy of glutamatergic synapses within the primary auditory cortex, associated with a major postsynaptic rearrangement compatible with an increase in the total number of synaptic connections.

Author statement

JN performed all the patch-clamp experiments, analyzed and elaborated data and figures, and contributed to writing the final version of the manuscript, VJ raised the EE animals and contributed to the discussion, LD wrote and ran the MatLab program using literature and original data, MK contributed to the original idea, to the design of the experiments and to the final version of the manuscript, MA contributed to the original idea and to the design of the experiments, and wrote the final version of the manuscript.

Grants: NIDCD 1R01-DC005986-01A1 and NARSAD foundation/Sidney Baer Trust (M.A.) and American Academy of Audiology to J.A.N.

Figure legends

Figure 1

AMPAR-mediated currents in Layer II/III. A and B. Mean traces for control (n = 10) and EE (n = 11) animals. C Intensity of the electrical stimulation for control (blank bar) and EE (gray bar) did not change. D Mean of the peak amplitude of the AMPAR-mediated current in control (blank bar, n = 10) vs. EE (gray bar, n = 11). The mean amplitude was more than 60% larger in EE animals. E Paired Pulse Ratio (PPR $=A_2/A_1$). PPR at an interpulse interval of 500 ms was smaller in EE animals (0.943 ± 0.026 in control vs 0.877 ± 0.018 in EE, n = 10 control; n = 11 in EE). F Rise time and G decay time of the eEPSC. The rise time is shorter in EE animals while no differences are present in the decay time. Altogether, these data suggest that EE elicits changes in glutamatergic synaptic signals.

Figure 2

Neurotransmitter- and layer-specificity of the synaptic changes. A, B, C and D: amplitude, rise time, decay time and PPR of GABAergic currents in layer II/III do not differ in control or in EE (n = 8 each). E, F, G and H: amplitude, rise time, decay time and PPR in AMPAR-mediated glutamatergic currents of layer V do not differ between control and EE (n = 5 control; n = 8 EE).

Figure 3

Invariance of the I_{NMDA}/I_{AMPA}. **A**. The AMPAR- and the NMDAR-dependent components of the glutamatergic currents were measured by recording a synaptic current at a holding voltage

V_h= -60 mV or V_h= +60 mV, the latter one to eliminate Mg^{+2} block. AMPA currents were measured, as elsewhere in the study, at the peak, NMDA currents were measured 45 ms after stimulation (arrow), to minimize any contamination by the AMPA component. B. Mean I_{NMDA}/I_{AMPA} in control (blank bar, n = 6) vs. EE animals (gray bar, n = 8). The parallel change in I_{NMDA} and I_{AMPA} supports the idea that EE induces a global increase in excitatory synaptic function.

Figure 4

Model of EE and enhanced gating. A simplistic model of cortical synaptic circuit with an input layer (P1), and output layer (P2) and an inhibitory interneuron (I1). Each model neuron represents a population of independent synaptic units. P1 receives two square current injections (10 ms - 100 ms between pulses) generating one action potential each. In the control situation none of the two synaptic responses generate an action potential in I1 (B, C, black line). In the EE only the second response generates an action potential in I1 (A and B, red lines), contributing to the decrease in PPR detected in vivo (D).

Figure 5

Enhanced robustness of EE synaptic summation. A: a second neural model simulated the effect of EE on the response to two oscillatory input, each separately below threshold. P3 is the output layer receiving input from two pyramidal cells receiving a subthreshold sinusoidal wave at the same frequency but with different phase. B, C and D: firing frequency variation in P3 for control (blue line) or EE (red line) at the input frequencies of 5, 20, or 50 Hz, as a function of the phase difference between the two inputs. At all frequencies a slight phase difference (< 30°) elicits an increase in the response due to longer interval for synaptic integration.

At high frequencies (i.e. 50 Hz) the only evident effect is the expected increase in frequency (B); at intermediate frequencies (20 Hz, C), a small phase difference increases the response, but the mean response is still heavily phase dependent in EE, vs. a flat phase dependence in control; at lower frequencies, where the input layer neurons (P1 and P2) have more time for synaptic integration, while in control only a small phase difference increases the response, in EE, the response increase are present almost in the full phase-difference interval.

Appendix

Pyramidal cell model

We represented the distribution of ionic currents across dendrites, soma and axon, in a three compartment pyramidal-cell model. The model includes the most relevant ionic conductances present in cortical pyramidal cells (Wang 1998): sodium (I_{Na}) current, delayed rectifier K^+ ($I_{K\text{-}dr}$) current, high-voltage activated Ca^{2+} (I_{Ca}) current, and a calcium-dependent K^+ current ($I_{K(Ca)}$). A coupling conductance (g_c) value regulates the current flow between dendrite and soma, and soma and axon. A slightly modified set of membrane conductances was used to describe interneuronal spiking. The somatic, dendritic, and axonal terminal membrane potentials V_s, V_d, and V_p are described by following equations

$$C_m \frac{dVs}{dt} = -I_L - I_{Na} - I_K - I_{Ca} - I_{AHP} + I_{inject} - \frac{gc}{p}(V_s - V_d)$$

$$C_m \frac{dVd}{dt} = -I_L - I_{Ca} - I_{AHP} - \frac{gc1}{(1-2*p)}(V_d - V_s) - I_{AMPA} - I_{NMDA}$$

$$C_m \frac{dVp}{dt} = -I_L - I_{Na} - I_K - I_{Ca} - I_{AHP} - \frac{gc2}{p}(V_p - V_s)$$

Where $C_m = 1\ \mu F/cm^2$ and I_{inject} is the cosine function (in $\mu A/cm^2$).

Short-term plasticity in a glutamatergic synapse:

The model contains four parameters representing the short-term dynamic of synaptic plasticity: facilitation (F), slow depression (DS), fast depression (DF) and initial amplitude (A_0). These four parameters are dependent on the intracellular calcium concentration. The change in response amplitude (A) is the product of these three parameters (Varela et al., 1997)

$$A = A_0 \cdot F \cdot DS \cdot DF$$

$$I_{AMPA(or\ NMDA)} = A \cdot \alpha(V) \cdot (V - E).$$

where $\alpha(V)$ is an α-function

$$\alpha(t) = t \cdot e^{-t/\tau}$$

where the kinetics of the glutamatergic synaptic currents is contained in the decay time τ (Brunel and Wang, 2001; Tiesinga and Sejnowski, 2001).

Reference List

Artola A, von Frijtag JC, Fermont PC, Gispen WH, Schrama LH, Kamal A, Spruijt BM, 2006. Long-lasting modulation of the induction of LTD and LTP in rat hippocampal CA1 by behavioural stress and environmental enrichment. Eur. J Neurosci 23: 261-272.

Atzori M, Flores HJ, Pineda JC, 2004. Interlaminar differences of spike activation threshold in the auditory cortex of the rat. Hear. Res. 189: 101-106.

Atzori M, Kanold PO, Pineda JC, Flores-Hernandez J, Paz RD, 2005. Dopamine prevents muscarinic-induced decrease of glutamate release in the auditory cortex. Neuroscience 134: 1153-1165.

Atzori M, Lei S, Evans DI, Kanold PO, Phillips-Tansey E, McIntyre O, McBain CJ, 2001. Differential synaptic processing separates stationary from transient inputs to the auditory cortex. Nat. Neurosci. 4: 1230-1237.

Bartoletti A, Medini P, Berardi N, Maffei L, 2004. Environmental enrichment prevents effects of dark-rearing in the rat visual cortex. Nat. Neurosci 7: 215-216.

Brunel N, Wang XJ, 2001. Effects of neuromodulation in a cortical network model of object working memory dominated by recurrent inhibition. J Comput. Neurosci 11: 63-85.

Dierssen M, avides-Piccione R, Martinez-Cue C, Estivill X, Florez J, Elston GN, DeFelipe J, 2003. Alterations of neocortical pyramidal cell phenotype in the Ts65Dn mouse model of Down syndrome: effects of environmental enrichment. Cereb. Cortex 13: 758-764.

Duffy SN, Craddock KJ, Abel T, Nguyen PV, 2001. Environmental enrichment modifies the PKA-dependence of hippocampal LTP and improves hippocampus-dependent memory. Learn. Mem. 8: 26-34.

Engineer ND, Percaccio CR, Pandya PK, Moucha R, Rathbun DL, Kilgard MP, 2004. Environmental enrichment improves response strength, threshold, selectivity, and latency of auditory cortex neurons. J Neurophysiol. 92: 73-82.

Faherty CJ, Kerley D, Smeyne RJ, 2003. A Golgi-Cox morphological analysis of neuronal changes induced by environmental enrichment. Brain Res. Dev. Brain Res. 141: 55-61.

Foster TC, Dumas TC, 2001. Mechanism for increased hippocampal synaptic strength following differential experience. J Neurophysiol. 85: 1377-1383.

Foster TC, Fugger HN, Cunningham SG, 2000. Receptor blockade reveals a correspondence between hippocampal-dependent behavior and experience-dependent synaptic enhancement. Brain Res. 871: 39-43.

Foster TC, Gagne J, Massicotte G, 1996. Mechanism of altered synaptic strength due to experience: relation to long-term potentiation. Brain Res. 736: 243-250.

Green EJ, Greenough WT, 1986. Altered synaptic transmission in dentate gyrus of rats reared in complex environments: evidence from hippocampal slices maintained in vitro. J Neurophysiol. 55: 739-750.

Hellemans KG, Nobrega JN, Olmstead MC, 2005. Early environmental experience alters baseline and ethanol-induced cognitive impulsivity: relationship to forebrain 5-HT1A receptor binding. Behav. Brain Res. 159: 207-220.

Irvine GI, Abraham WC, 2005. Enriched environment exposure alters the input-output dynamics of synaptic transmission in area CA1 of freely moving rats. Neurosci Lett. 391: 32-37.

Isaac JT, Nicoll RA, Malenka RC, 1999. Silent glutamatergic synapses in the mammalian brain. Can. J Physiol Pharmacol. 77: 735-737.

Johansson BB, Belichenko PV, 2002. Neuronal plasticity and dendritic spines: effect of environmental enrichment on intact and postischemic rat brain. J Cereb. Blood Flow Metab 22: 89-96.

Leggio MG, Mandolesi L, Federico F, Spirito F, Ricci B, Gelfo F, Petrosini L, 2005. Environmental enrichment promotes improved spatial abilities and enhanced dendritic growth in the rat. Behav. Brain Res. 163: 78-90.

Nithianantharajah J, Levis H, Murphy M, 2004. Environmental enrichment results in cortical and subcortical changes in levels of synaptophysin and PSD-95 proteins. Neurobiol. Learn. Mem. 81: 200-210.

Percaccio CR, Engineer ND, Pruette AL, Pandya PK, Moucha R, Rathbun DL, Kilgard MP, 2005. Environmental enrichment increases paired-pulse depression in rat auditory cortex. J Neurophysiol. 94: 3590-3600.

Sharp PE, McNaughton BL, Barnes CA, 1985. Enhancement of hippocampal field potentials in rats exposed to a novel, complex environment. Brain Res. 339: 361-365.

Tiesinga PH, Sejnowski TJ, 2001. Precision of pulse-coupled networks of integrate-and-fire neurons. Network. 12: 215-233.

Varela JA, Sen K, Gibson J, Fost J, Abbott LF, Nelson SB, 1997. A quantitative description of short-term plasticity at excitatory synapses in layer 2/3 of rat primary visual cortex. J Neurosci 17: 7926-7940.

Wang XJ, 1998. Calcium coding and adaptive temporal computation in cortical pyramidal neurons. J Neurophysiol. 79: 1549-1566.

Zhu J, Apparsundaram S, Bardo MT, Dwoskin LP, 2005. Environmental enrichment decreases cell surface expression of the dopamine transporter in rat medial prefrontal cortex. J Neurochem. 93: 1434-1443.

4 - Table

Table 1 : The average number of spikes in the intervals of 0-30 degree and 31-180 degree phase difference, respectively; and their ratio ($2^{nd}/1^{st}$ interval).

		50 Hz			**20 Hz**			**5 Hz**		
ΔPhase		0-30	31-180	Ratio	0-30	31-180	Ratio	0-30	31-180	Ratio
Firing Frequency	**Control (CE)**	3.0	2.9	**0.97**	5.0	5.0	**1.00**	7.1	5.9	**0.83**
	Enriched (EE)	5.4	5.7	**1.06**	7.4	8.2	**1.11**	8.9	10.5	**1.18**

Figure 1

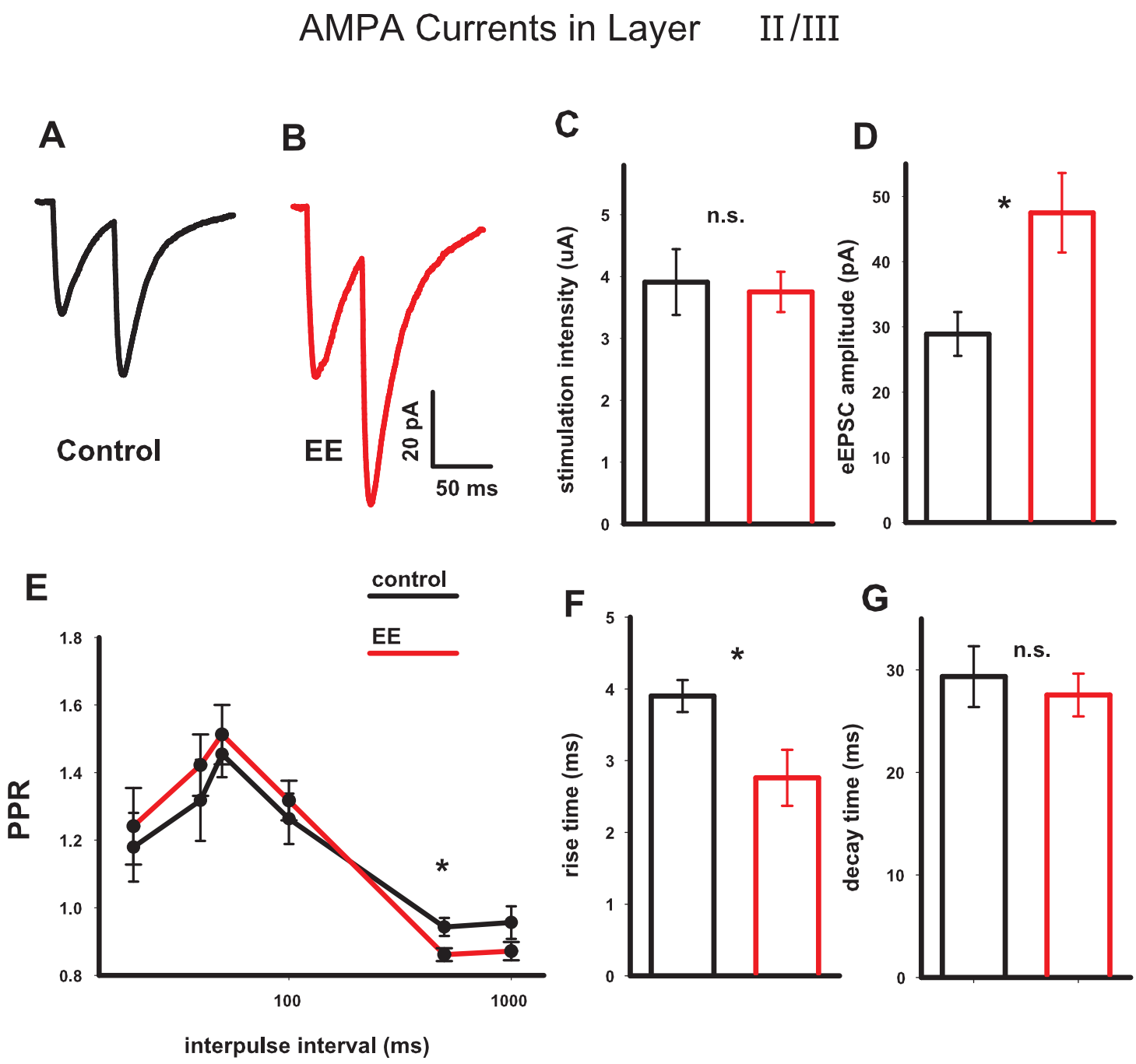
AMPA Currents in Layer II/III
A
Control
B
EE
20 pA
50 ms
C
stimulation intensity (uA)
n.s.
D
eEPSC amplitude (pA)
*
E
control
EE
PPR
*
interpulse interval (ms)
F
rise time (ms)
*
G
decay time (ms)
n.s.

Figure 2

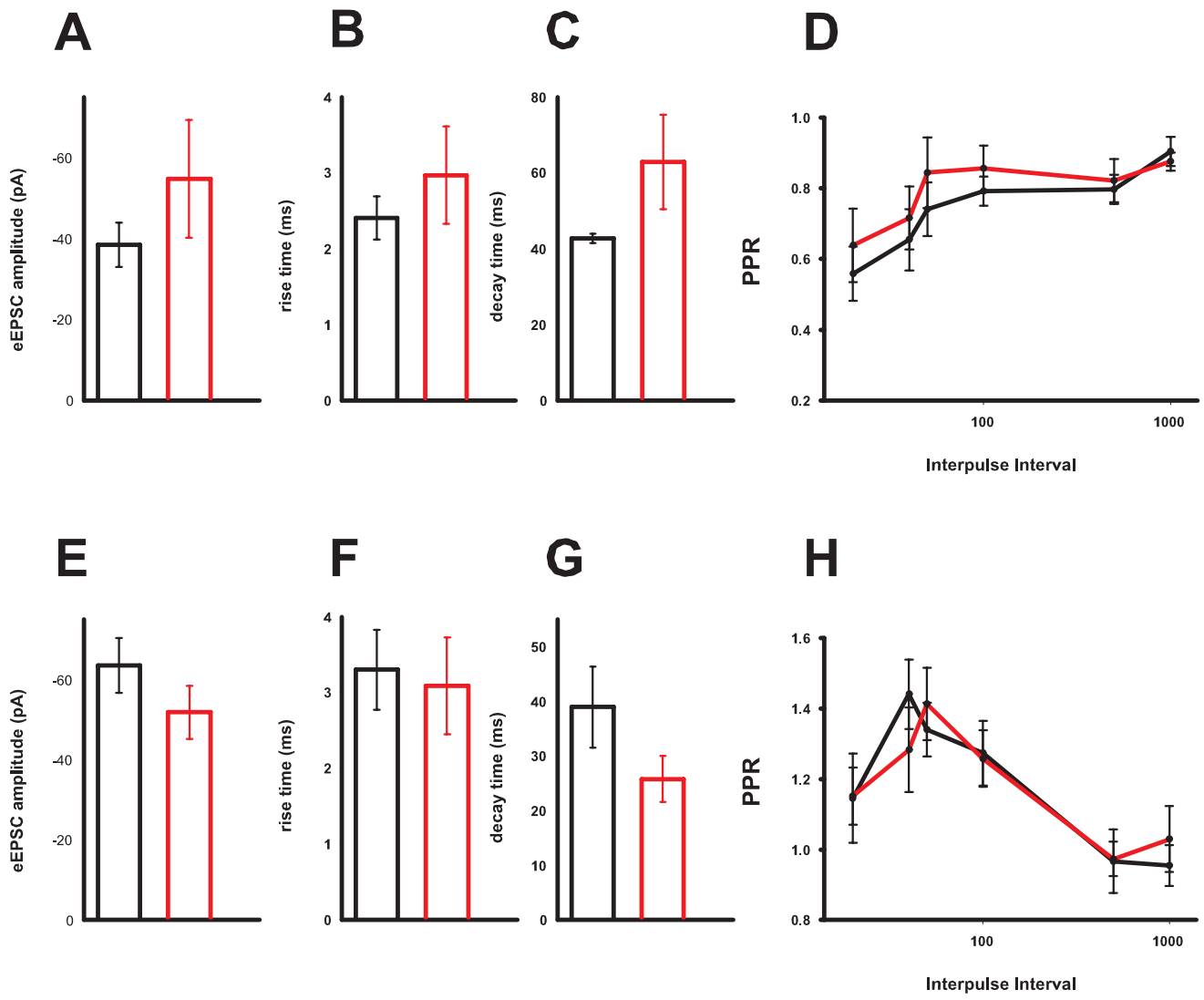
A
B
C
D
eEPSC amplitude (pA)
0
-20
-40
-60
rise time (ms)
0
1
2
3
4
decay time (ms)
0
20
40
60
80
PPR
0.2
0.4
0.6
0.8
1.0
100
1000
Interpulse Interval
E
F
G
H
eEPSC amplitude (pA)
0
-20
-40
-60
rise time (ms)
0
1
2
3
4
decay time (ms)
0
10
20
30
40
50
PPR
0.8
1.0
1.2
1.4
1.6
100
1000
Interpulse Interval

Figure 3

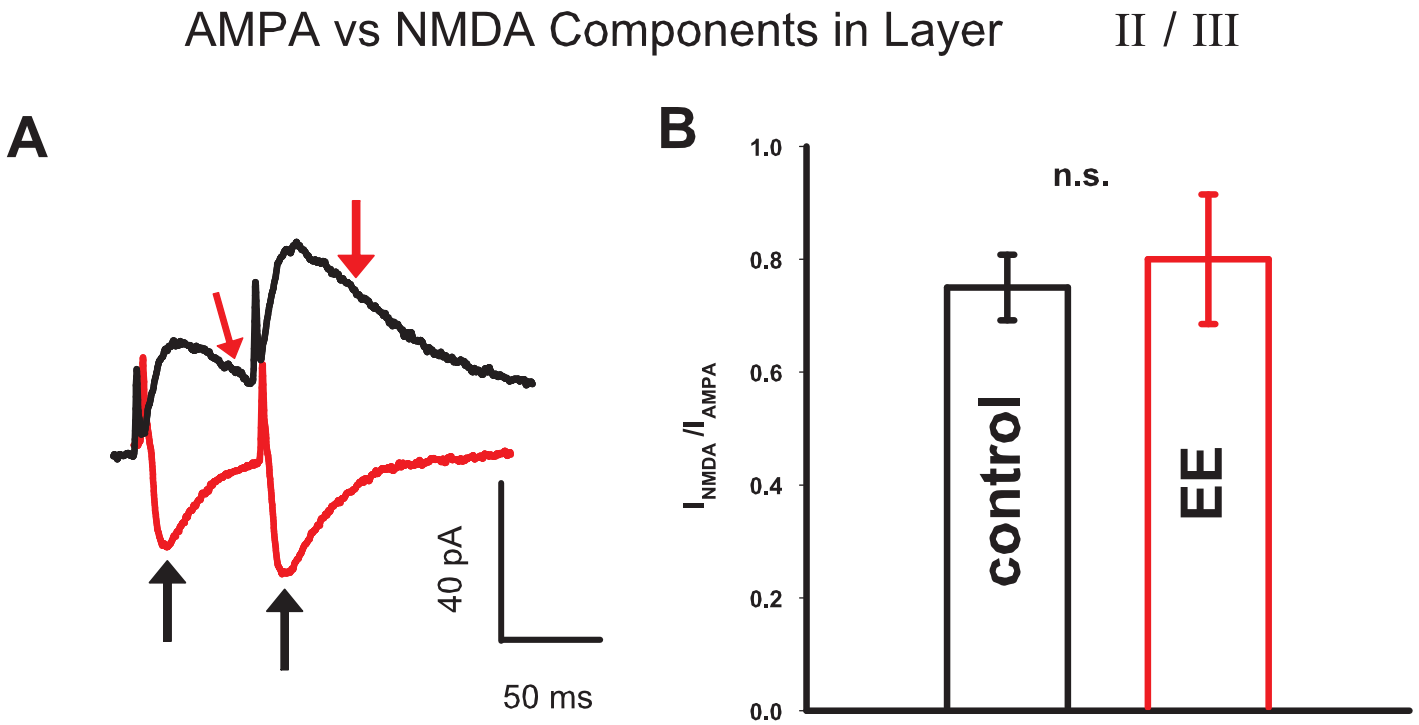
AMPA vs NMDA Components in Layer II / III
A
40 pA
50 ms
B
n.s.
1.0
0.8
0.6
0.4
0.2
0.0
I_NMDA /I_AMPA
control
EE

Figure 4

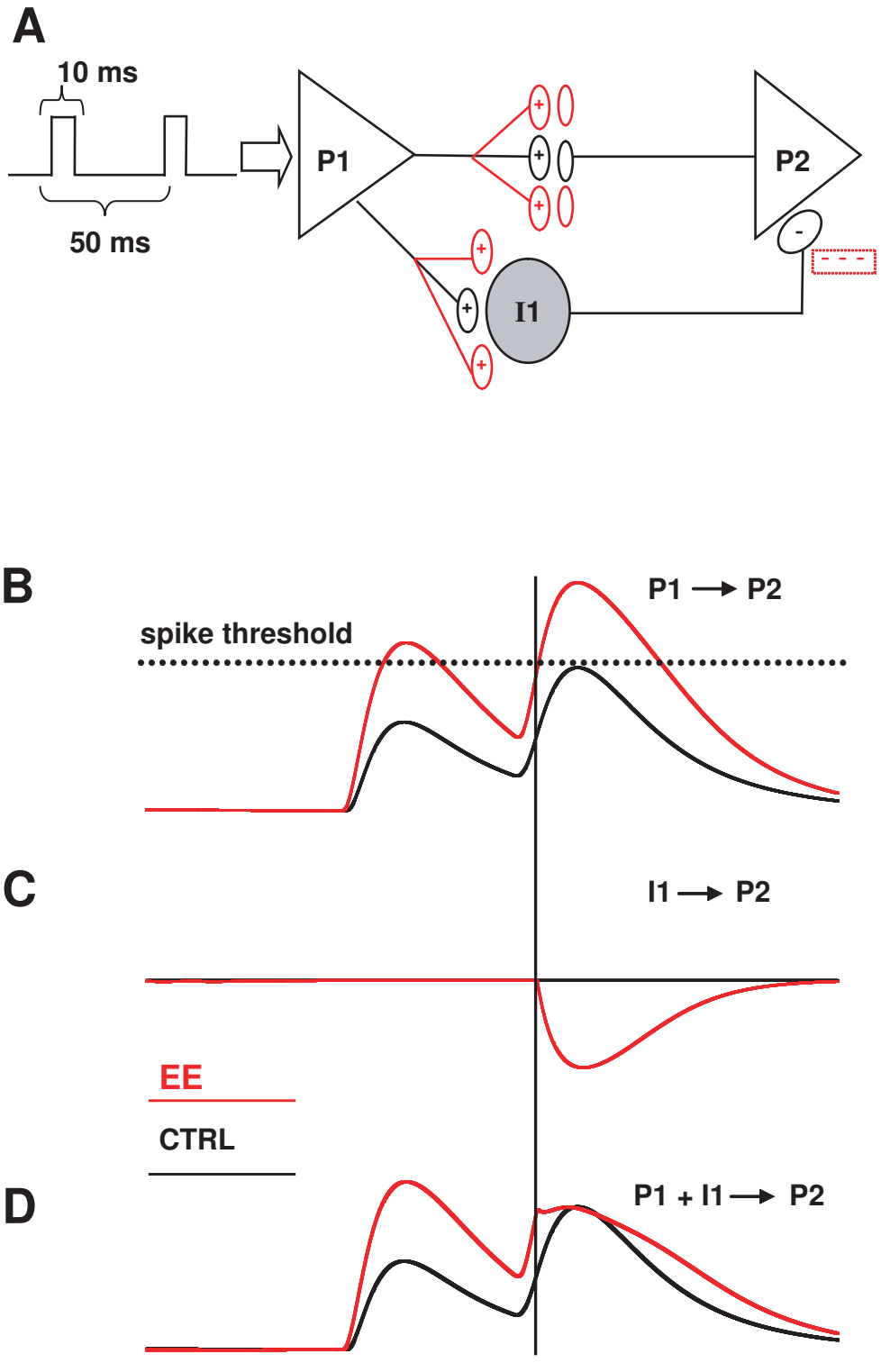
A
10 ms
50 ms
P1
P2
I1
B
P1 → P2
spike threshold
C
I1 → P2
EE
CTRL
D
P1 + I1 → P2

Figure 5

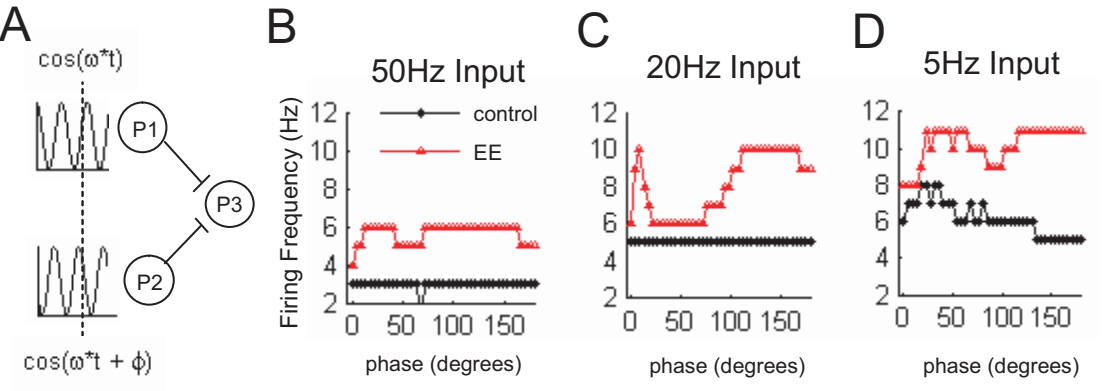
A
cos(ω*t)
P1
P3
P2
cos(ω*t + ϕ)
B
50Hz Input
control
EE
Firing Frequency (Hz)
12
10
8
6
4
2
0
50
100
150
phase (degrees)
C
20Hz Input
phase (degrees)
D
5Hz Input
phase (degrees)